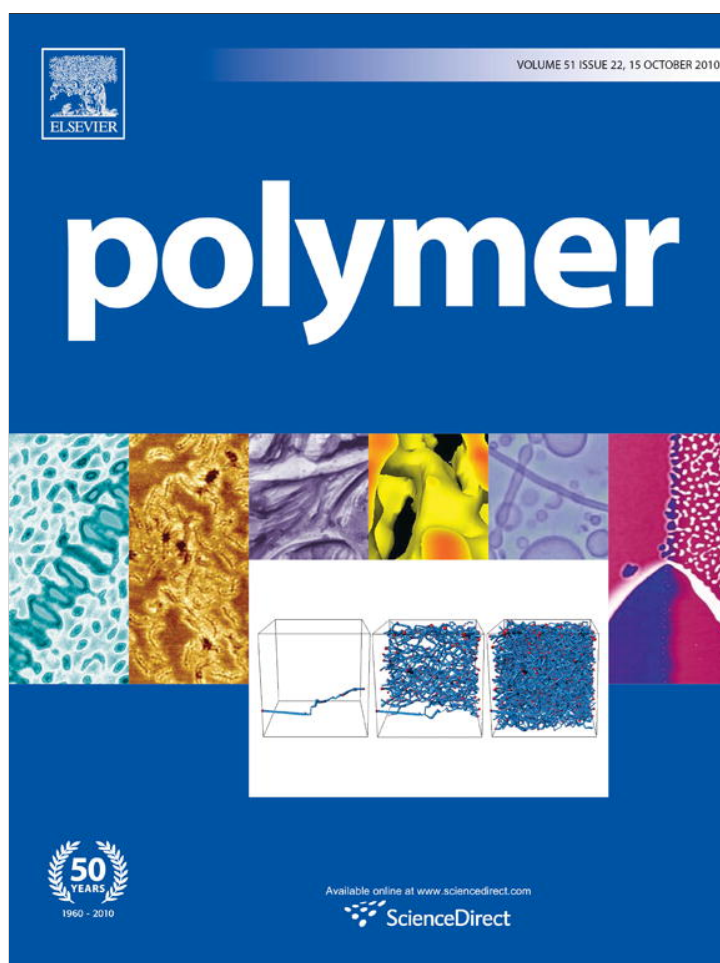


Provided for non-commercial research and education use.  
Not for reproduction, distribution or commercial use.

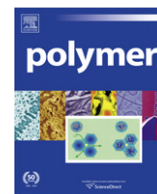


This article appeared in a journal published by Elsevier. The attached copy is furnished to the author for internal non-commercial research and education use, including for instruction at the authors institution and sharing with colleagues.

Other uses, including reproduction and distribution, or selling or licensing copies, or posting to personal, institutional or third party websites are prohibited.

In most cases authors are permitted to post their version of the article (e.g. in Word or Tex form) to their personal website or institutional repository. Authors requiring further information regarding Elsevier's archiving and manuscript policies are encouraged to visit:

<http://www.elsevier.com/copyright>



# A dual mode interpretation of the kinetics of penetrant-induced swelling and deswelling in a glassy polymer

Juchen Guo<sup>a</sup>, Timothy A. Barbari<sup>b,\*</sup>

<sup>a</sup> Department of Chemical and Biomolecular Engineering, University of Maryland, College Park, MD 20742, USA

<sup>b</sup> Department of Physics, Georgetown University, Washington, DC 20057, USA

## ARTICLE INFO

### Article history:

Received 29 June 2010

Received in revised form

23 August 2010

Accepted 27 August 2010

Available online 8 September 2010

### Keywords:

Glassy polymer

Swelling

Kinetics

## ABSTRACT

In this study, a unified dual mode description of penetrant sorption and desorption kinetics in a glassy polymer was extended to the study of the kinetics of penetrant-induced swelling and deswelling below the glass transition concentration. The swelling of cellulose acetate (CA) induced by the sorption of vapor phase acetonitrile, and the subsequent deswelling during desorption, was measured using time-resolved FTIR-ATR (Fourier Transform Infrared-Attenuated Total Reflectance) spectroscopy. Equilibrium swelling as a function of penetrant activity from the spectroscopic measurements was confirmed with conventional length elongation measurements (dilatometry). From equilibrium measurements that traversed the glass transition concentration, the partial molar volume both below and above the transition was determined. Using the partial molar volume obtained above the glass transition and assuming that only the dissolved population contributes to dilation, the swelling kinetics can be predicted from the dual mode framework presented here. However, the deswelling kinetics cannot be predicted, suggesting that a fraction of the holes formed upon sorption in the unified model must collapse during contraction of the polymer upon desorption.

© 2010 Elsevier Ltd. All rights reserved.

## 1. Introduction

FTIR-ATR spectroscopy is finding increased use as a tool to study the sorption and transport of penetrants in polymers [1]. However, there have been considerably fewer studies that utilize the unique capability of FTIR-ATR spectroscopy to study penetrant-induced polymer swelling. Balik and Xu studied the swelling of latex paint induced by the sorption of water [2]. In their study, the extent of swelling was determined from the decrease in the local infrared absorbance of the C–H stretch and confirmed by a direct volume measurement. Sammon et al. [3] used FTIR-ATR spectroscopy to study the swelling of a poly(ethylene terephthalate) film upon the sorption of methanol. Baschetti et al. [4] studied the swelling of three different polymers, polycarbonate, poly(vinyl acetate) and poly(ether urethane), induced by the sorption of vapor phase acetonitrile. In their study, direct volume change measurements were compared to FTIR-ATR dilation data, with excellent agreement between the two techniques. The equilibrium swelling data were fit with lattice fluid models. In each of these previous studies, the emphasis was on using FTIR-ATR spectroscopy to examine the equilibrium swelling in these materials.

In the present study, the swelling kinetics of cellulose acetate (CA) films, induced by the sorption of vapor phase acetonitrile, were measured using FTIR-ATR spectroscopy at various penetrant activities. The corresponding deswelling kinetics were also measured during desorption. Predictions of the swelling and deswelling behavior were made using a unified dual mode model, proposed by the authors in a previous study [5], and compared to the actual FTIR-ATR swelling and deswelling data. The model used here was developed by the authors to remove the discontinuities inherent in the classic dual mode model in the concentrations of both the dissolved and hole populations between sorption at a particular activity and desorption initiation at that same activity.

The classic dual mode sorption model is given by

$$C = C_D + C_H = k_D a + C'_H \frac{ba}{1 + ba} \quad (1)$$

where  $C_D$  and  $C_H$  are the concentrations of the dissolved and hole populations, respectively,  $k_D$  is the Henry's law constant,  $a$  is the penetrant activity in the vapor phase,  $C'_H$  is the Langmuir capacity, and  $b$  is the Langmuir affinity constant. Sorption and desorption isotherms for acetonitrile in cellulose acetate are shown in Fig. 1. Applying Eq. (1) to the desorption isotherms below the glass transition concentration for the acetonitrile–cellulose acetate system, keeping  $b$  for desorption equal to that for sorption, results

\* Corresponding author. Tel.: +1 202 687 5603; fax: +1 202 687 6802.  
E-mail address: [tab53@georgetown.edu](mailto:tab53@georgetown.edu) (T.A. Barbari).

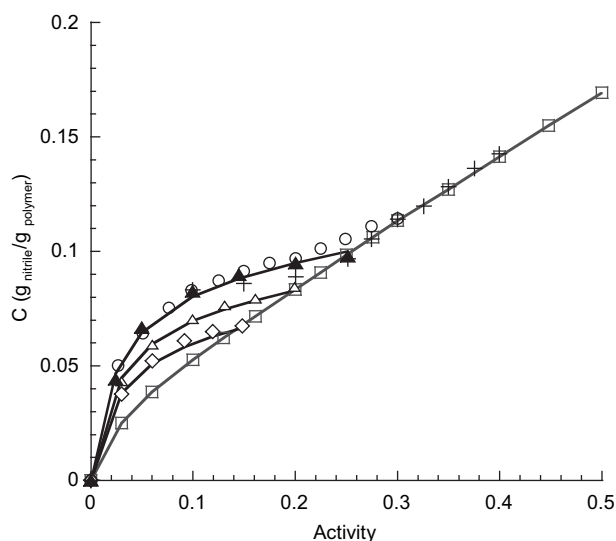


**Fig. 1.** Acetonitrile sorption isotherm (open squares) and desorption initiation isotherms at activities of 0.15 (open diamonds), 0.20 (open triangles), 0.25 (solid triangles), 0.30 (open circles) and 0.40 (crosses) at  $T = 25\text{ }^{\circ}\text{C}$ . The solid lines represent dual mode model fits using Eqs. (1)–(3).

in values of  $k_D$  that, on average, are considerably lower than the  $k_D$  for sorption [5]. As expected from the shapes of the desorption isotherms, the values of  $C_H$  for desorption are dependent on the starting activity from which the desorption isotherm is measured. At a given activity along the sorption isotherm,  $C_D$  and  $C_H$  can be calculated from the classic dual mode parameters applied to that isotherm. If the same calculation is made using the parameters obtained from the desorption isotherm at that activity, radically different concentrations result. This implies that the two populations must instantaneously redistribute themselves between the end of sorption and the beginning of desorption, which is difficult to explain physically in the context of modeling sorption and desorption kinetics.

In an effort to eliminate this discontinuity, an alternative physical picture of sorption and desorption in glassy polymers was proposed in our previous paper [5]. The basic premise is that a fraction of the dissolved population from the classic model forms new occupied holes during sorption leading to a continuous redistribution of the two populations as a function of local activity. These holes would then remain during desorption assuming that the time scale for any chain relaxation is longer than that for diffusion. If  $f_H$  represents the fraction of the dissolved population in the classic framework that forms new holes, then the dual mode sorption model can be recast as [5]

$$C = C_D^* + C_H^* = [(1 - f_H)C_D] + [C_H + f_H C_D] \\ = (1 - f_H)k_D a + C_{H0} \left( 1 + \eta \frac{1 + ba}{b} \right) \frac{ba}{1 + ba} \quad (2)$$

where  $\eta = f_H k_D / C_{H0}$  and  $C_{H0}$  is the pre-existing Langmuir capacity for the as-prepared polymer. If the newly formed holes do not collapse during desorption, then the analogous expression for the desorption isotherm starting at activity  $a_d$  is given by

$$C = (1 - f_H)k_D a + C_{H0} \left( 1 + \eta \frac{1 + ba_d}{b} \right) \frac{ba}{1 + ba} \quad (3)$$

Applying Eqs. (1)–(3) to the sorption and desorption isotherms results in the curves shown in Fig. 1 with  $k_D = 0.282\text{ g}_{\text{nitrile}}/\text{g}_{\text{polymer}}$ ,  $b = 38.1$ ,  $f_H = 0.79$ , and  $C_{H0} = 0.030\text{ g}_{\text{nitrile}}/\text{g}_{\text{polymer}}$  [5].

A companion transport model can be written based on  $C_D^*$  as the only mobile population for sorption and desorption kinetics. According to this unified dual mode model, sorption kinetics can be described by [5]:

$$\frac{\partial C}{\partial t} = D_D \frac{\partial}{\partial z} \left[ \frac{1}{1 + \frac{S + 2\delta C_D^* + \beta \delta C_D^{*2}}{(1 + \beta C_D^*)^2}} \frac{\partial C}{\partial z} \right] \quad (4)$$

where

$$C_D^* = \frac{-(1 + S - \beta C) + [(1 + S - \beta C)^2 + 4(\beta + \delta)C]^{1/2}}{2(\beta + \delta)}$$

$$\beta = \frac{b}{(1 - f_H)k_D}$$

$$S = \beta \left( C_{H0}' + \frac{f_H k_D}{b} \right)$$

$$\delta = \frac{f_H}{(1 - f_H)}$$

For desorption kinetics, the model is:

$$\frac{\partial C}{\partial t} = D_D \frac{\partial}{\partial z} \left[ \frac{1}{1 + \frac{K}{(1 + \alpha C_D^*)^2}} \frac{\partial C}{\partial z} \right] \quad (5)$$

where

$$C_D^* = \frac{-(1 + K - \alpha C) + [(1 + K - \alpha C)^2 + 4\alpha C]^{1/2}}{2\alpha}$$

$$\alpha = \frac{b}{(1 - f_H)k_D}$$

$$K = \frac{C_{Hd}' b}{(1 - f_H)k_D}$$

$$C_{Hd}' = C_{H0}' + f_H k_D a_d$$

When Eqs. (4) and (5) were applied to sorption and desorption kinetics data, respectively, in the previous study [5], better agreement between sorption and desorption diffusion coefficients at a given activity were obtained, in contrast to the application of a transport model based on the classic dual mode model. The diffusion coefficients from the unified model for sorption and desorption kinetics for the acetonitrile/CA system are listed in Table 1.

**Table 1**  
Diffusion coefficients from the unified model for sorption and desorption kinetics for acetonitrile in CA at 25 °C.

Activity	$D_D \times 10^9\text{ cm}^2/\text{s}$	
	Sorption	Desorption
0.06	0.90 ± 0.05	0.95 ± 0.02
0.10	1.43 ± 0.06	1.82 ± 0.35
0.15	2.21 ± 0.12	3.45 ± 0.005
0.20	3.12 ± 0.08	6.70 ± 0.74
0.25	3.54 ± 0.42	10.44 ± 1.06

## 2. Materials and methods

### 2.1. Sample preparation for elongation measurements

In this study, a narrow polymer strip was prepared for the measurement of film elongation at equilibrium sorption, from which volumetric dilation could be calculated. Acetonitrile ( $\text{CH}_3\text{CN}$ ) and cellulose acetate (39.8 wt.% acetyl content, average mol wt  $\sim 30,000$ ) were purchased from Sigma–Aldrich and used as received. The details of film casting were described previously [5]. The film was prepared on a glass slide ( $7.5 \text{ cm} \times 2 \text{ cm}$ ). After carefully peeling it from the glass slide, the film was cut into a rectangular strip ( $2 \text{ cm} \times 0.5 \text{ cm}$ ). To measure the elongation during sorption, the polymer strip was hung on a hook inside the vapor sorption chamber described previously [5], with a 0.10 g weight fixed at the lower end of the strip to prevent curling. The elongation in the film upon vapor sorption was measured using a cathetometer, as a function of activity. At each activity, the strip was exposed to acetonitrile vapor for 48 h to ensure equilibrium swelling.

### 2.2. Swelling measurements and analysis

The swelling of cellulose acetate during the sorption of vapor phase acetonitrile was measured by either direct observation of sample elongation with a cathetometer (equilibrium swelling) or monitoring the carbonyl ( $\text{C}=\text{O}$ ) stretching peak in the polymer with the FTIR-ATR technique (equilibrium swelling and swelling kinetics). In our previous study [5], sorption and desorption kinetics were monitored through the nitrile stretching band in acetonitrile. In those experiments, the carbonyl stretching band was also tracked in real time for subsequent analysis here. Details on the FTIR-ATR experiments themselves were described previously [5]. The volume change,  $\Delta V$ , of the CA films at equilibrium can be expressed in terms of the elongation,  $L$  [6]:

$$\frac{\Delta V}{V_0} = \left(\frac{L}{L_0}\right)^3 - 1 = \left(1 + \frac{\Delta L}{L_0}\right)^3 - 1 \quad (6)$$

where  $V_0$  and  $L_0$  are the volume and length of the pure polymer strip, respectively. The extent of swelling, as calculated from Eq. (6) from the elongation data, is plotted as a function of activity in Fig. 2.

## 3. Results and discussion

### 3.1. Partial molar volume of acetonitrile in CA

In order to make predictions of the kinetics of swelling from sorption kinetics and measured diffusion coefficients, a relationship

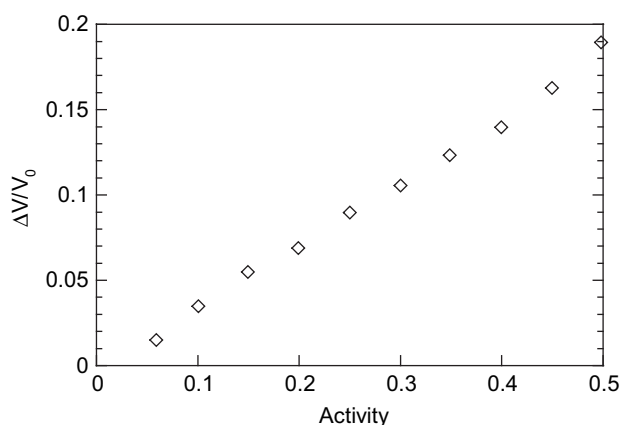


Fig. 2. Swelling of CA by acetonitrile as a function of activity at  $T = 25 \text{ }^\circ\text{C}$ .

between concentration and volume dilation is required. For rubbery polymers, the relationship is typically linear and assumes a constant partial molar volume of the penetrant. For glassy polymers, the presence of unrelaxed free volume, or holes, results in penetrant being sorbed with little to no dilation of the polymer. If one assumes that the hole population does not contribute to swelling and that the dissolved population contributes by an amount equal to its partial molar volume in the rubbery state, then determining this volume is the first step in making predictions of swelling kinetics. Combining measurements of acetonitrile mass uptake and swelling at equilibrium sorption allows one to use a straightforward thermodynamic approach to determine the partial molar volume of acetonitrile in CA [7,8].

For a binary system such as acetonitrile/CA, the partial specific volumes of CA and acetonitrile can be expressed as:

$$v_1 = v_t - \omega_2 \left( \frac{dv_t}{d\omega_2} \right) \quad (7)$$

$$v_2 = v_t + (1 - \omega_2) \left( \frac{dv_t}{d\omega_2} \right) \quad (8)$$

where  $v_1$  and  $v_2$  are the partial specific volumes of the CA and acetonitrile, respectively,  $v_t$  is the total specific volume of the system, and  $\omega_2$  is the acetonitrile mass fraction. Hence, the partial specific volume of the acetonitrile can be determined from the slope of the total specific volume of the acetonitrile/CA system plotted against the mass fraction of acetonitrile. The total specific volume of the system and the mass fraction of acetonitrile, respectively, can be written as:

$$v_t = \frac{V_0 + \Delta V}{C(V_0\rho_{\text{poly}}) + V_0\rho_{\text{poly}}} = \frac{1 + \Delta V/V_0}{\rho_{\text{poly}}(1 + C)} \quad (9)$$

$$\omega_{\text{nitrile}} = \frac{C\rho_{\text{poly}}V_0}{C\rho_{\text{poly}}V_0 + \rho_{\text{poly}}V_0} = \frac{C}{1 + C} \quad (10)$$

where  $C$  is the acetonitrile concentration in CA at equilibrium (in  $\text{g}_{\text{nitrile}}/\text{g}_{\text{poly}}$ ), which is shown in Fig. 1 as a function of activity, and  $\rho_{\text{poly}}$  is the density of the pure CA polymer.

The density of the as-received CA is  $1.3 \text{ g/cm}^3$ , as provided by the supplier. However, CA film density may depend on the film formation process. Based on a study of Puleo and Paul [9], who measured the density of a CA film that was similar to that used in the present study (39.8 wt% acetyl content and 2.45 Degree of Substitution) and the same solution-casting method (acetone as

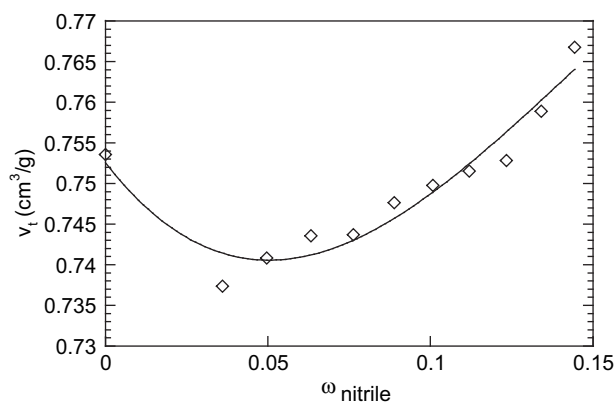


Fig. 3. Total specific volume of the acetonitrile/CA system as a function of acetonitrile mass fraction.  $T = 25 \text{ }^\circ\text{C}$ .

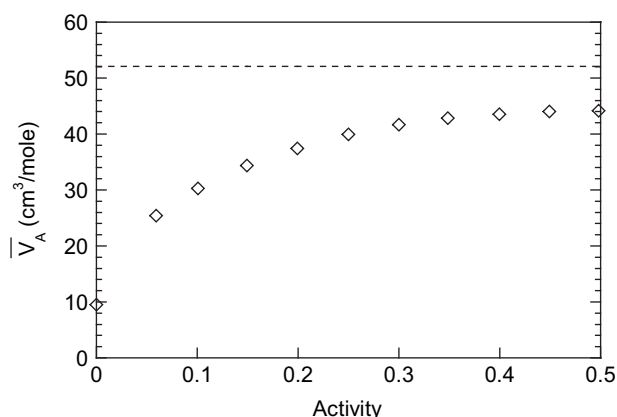


Fig. 4. Partial molar volume of acetonitrile in the acetonitrile/CA system as a function of activity at  $T = 25\text{ }^{\circ}\text{C}$ . The dashed line represents the molar volume of pure acetonitrile.

solvent), the resulting polymer film density was  $1.327\text{ g/cm}^3$ . Using this value, the specific volume of the acetonitrile/CA system was plotted as a function of mass fraction of acetonitrile, as shown in Fig. 3. This figure shows the expected trend of total specific volume for a glassy polymer first decreasing as unoccupied volume is filled and then increasing above the glass transition concentration in the rubbery state [8]. Eq. (8) was then used to determine the partial specific volume of acetonitrile in the system. One can convert from partial specific volume to partial molar volume by simply multiplying the former by the molecular weight of acetonitrile,  $41\text{ g/mol}$ . The partial molar volume of acetonitrile in the acetonitrile/CA system is plotted as a function of activity in Fig. 4. As indicated in this figure, the partial molar volume of acetonitrile is concave to the activity axis, and asymptotically approaches a value of  $44\text{ cm}^3/\text{mol}$ . As was discussed in our previous study [5] and as depicted in Fig. 1, the acetonitrile/CA system is in a rubbery state at activities 0.4 and 0.5. Therefore, the partial molar volume of acetonitrile at these activities should correspond to a value expected for liquids or rubbery polymers. From Baschetti et al. [4], the partial molar volume of acetonitrile in poly(vinyl acetate) and poly(ether urethane), both rubbery polymers, was determined to be 43 and  $42\text{ cm}^3/\text{mol}$ , respectively. The value calculated in the present study compares well to those values and will be used below to relate  $C_D^*$  to the extent of swelling.

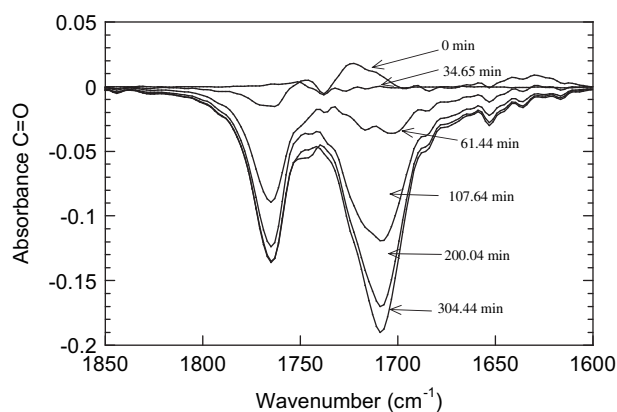


Fig. 5. Time-resolved carbonyl absorbance spectra in cellulose acetate at activity 0.2 and  $T = 25\text{ }^{\circ}\text{C}$  shown as differences relative to the pure polymer.

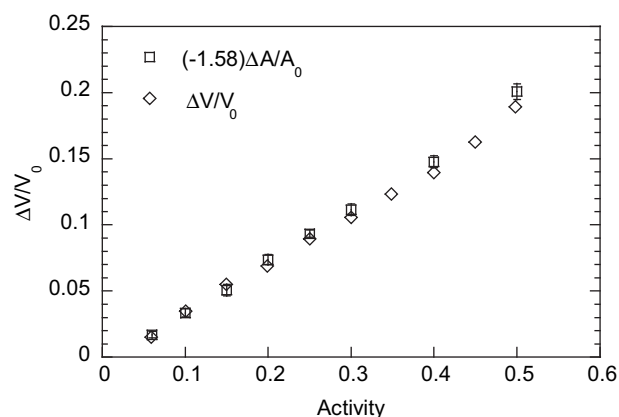


Fig. 6. Swelling from both direct measurement and FTIR-ATR absorbance as a function of activity.

### 3.2. Polymer swelling as measured by FTIR-ATR

When the polymer swells during penetrant sorption, the local concentration of polymer chains decreases such that the number of local polymer functional groups that can absorb IR radiation is also lowered. In this study, the characteristic functional group used for monitoring the swelling of cellulose acetate is the carbonyl group,  $\text{C}=\text{O}$ , from wavenumber  $1600\text{ cm}^{-1}$  to wavenumber  $1850\text{ cm}^{-1}$ . A representative series of time-resolved absorbance spectra for the carbonyl group during the swelling of a CA film is shown in Fig. 5. The spectrum of the pure polymer has been subtracted from each time point to highlight the decrease in  $\text{C}=\text{O}$  groups upon sorption. The presence of two  $\text{C}=\text{O}$  peaks reflects free and hydrogen-bound states within the polymer. Hydrogen bonding occurs with available OH groups in CA, which can also hydrogen bond with the sorbed acetonitrile.

If changes in the polymer functional group being monitored for swelling are relatively minor and if the sample is taken as non-constrained, then one can assume a linear relationship between the dilution of the IR absorbance of a polymer peak and the polymer dilation [4]:

$$\frac{\Delta V}{V_0} = -\frac{\Delta A}{A_0} \quad (11)$$

where  $\Delta A$  and  $\Delta V$  represent the changes in IR absorbance and sample volume, respectively, relative to their pure polymer values,

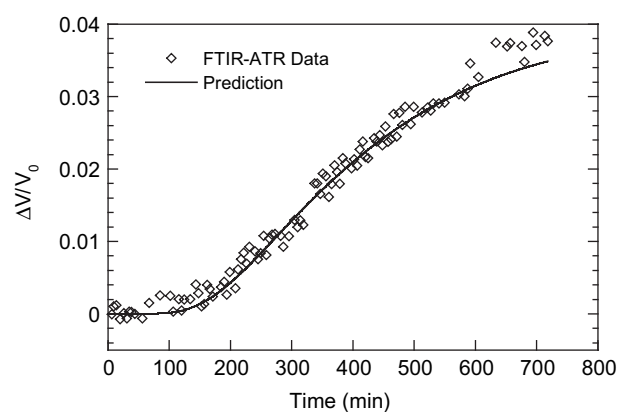


Fig. 7. FTIR-ATR swelling kinetics data and the prediction from the unified dual mode model at activity 0.1.  $L = 29.8\text{ }\mu\text{m}$  and  $T = 25\text{ }^{\circ}\text{C}$ .

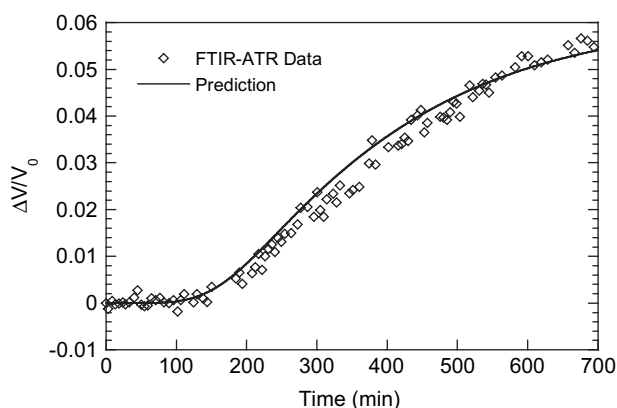


Fig. 8. FTIR-ATR swelling kinetics data and the prediction from the unified dual mode model at activity 0.15,  $L = 38.4 \mu\text{m}$  and  $T = 25^\circ\text{C}$ .

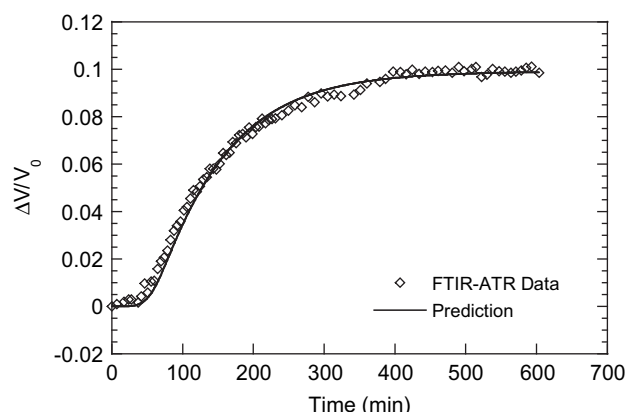


Fig. 10. FTIR-ATR swelling kinetics data and the prediction from the unified dual mode model at activity 0.25,  $L = 30.4 \mu\text{m}$  and  $T = 25^\circ\text{C}$ .

$A_0$  and  $V_0$ . However, in the FTIR-ATR experimental arrangement [5], the films are constrained from swelling in-plane (attached to the ATR crystal) and only out-of-plane swelling occurs. The relationship between changes in the IR absorbance and the extent of swelling for the constrained film was developed by Baschetti et al. [4] and can be written as:

$$\frac{\Delta V}{V_0} = -\frac{3(1-\nu)}{\nu+1} \frac{\Delta A}{A_0} \quad (12)$$

where  $\nu$  is the Poisson ratio for cellulose acetate.

The Poisson ratio for cellulose acetate can be calculated from the relationship between bulk modulus,  $B$ , and Young's modulus,  $E$ :

$$E = 3B(1 - 2\nu) \quad (13)$$

The Young's modulus for cellulose acetate is 2 GPa [10], and the bulk modulus can be estimated from Ref. [10]

$$B = (\mathbf{U}/\mathbf{V})^6 \rho_{\text{poly}} \quad (14)$$

where  $\mathbf{U}$  is the Rao function or molar sound velocity function and  $\mathbf{V}$  is the molar volume per structural unit of cellulose acetate (or  $M/\rho_{\text{poly}}$ , where  $M = 678.6$ , the molecular weight of the structural unit of cellulose acetate). Using a group contribution method, the Rao function was calculated to be  $\mathbf{U} = 24,860$ . From the density of the CA film,  $1.327 \text{ g/cm}^3$ ,  $\mathbf{V} = 511.4 \text{ cm}^3/\text{mol}$ . The resulting bulk modulus was calculated from Eq. (14):  $B = 1.75 \text{ GPa}$ . The Poisson

ratio calculated from Eq. (13) was 0.31. Thus, the constrained swelling data obtained from the C=O band in the FTIR-ATR experiments was multiplied by a factor of  $-1.58$  for comparison with the unconstrained direct swelling measurement for the free sample. The average of reported Poisson ratios for cellulose acetate was found to be 0.30 [11], which is in good agreement with the value calculated above.

The FTIR-ATR absorbance of the carbonyl group in the pure polymer,  $A_0$ , was obtained by integrating the carbonyl region of a pure CA film. The mean value of  $A_0$ , from 10 experiments, was  $80.0 \pm 1.9$ . The change in the absorbance of the carbonyl group as a function of activity, at equilibrium, was obtained by integration of the carbonyl region at each activity. The swelling data obtained from the FTIR-ATR experiments are plotted in Fig. 6 alongside those from direct measurement of elongation. The two methods are in excellent agreement. These results indicate that the FTIR-ATR technique can be a powerful alternative for the measurement of polymer swelling, particularly *in situ* with vapor or liquid penetrants.

### 3.3. Study of swelling kinetics by FTIR-ATR

The unified dual mode sorption model, Eq. (2), can be rewritten in the form:

$$C = C_D^* + \frac{C'_{H0}ba}{1+ba} + C_D^* \frac{f_H}{1-f_H} \quad (15)$$

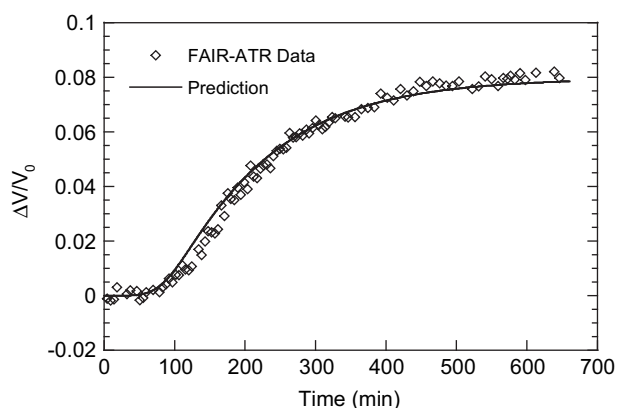


Fig. 9. FTIR-ATR swelling kinetics data and the prediction from the unified dual mode model at activity 0.2,  $L = 34.2 \mu\text{m}$  and  $T = 25^\circ\text{C}$ .

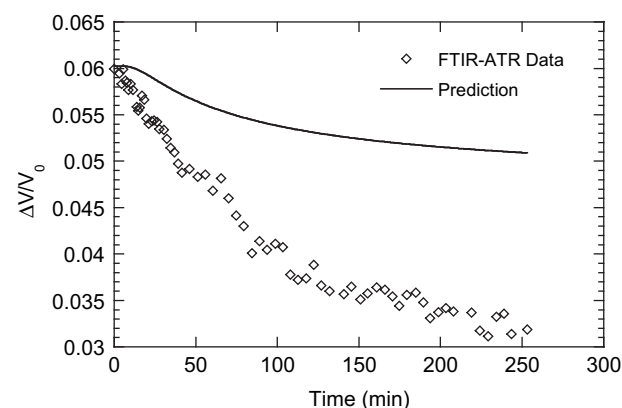


Fig. 11. Prediction of deswelling FTIR-ATR data at activity 0.15 with Eq. (17).  $L = 38.4 \mu\text{m}$  and  $T = 25^\circ\text{C}$ .

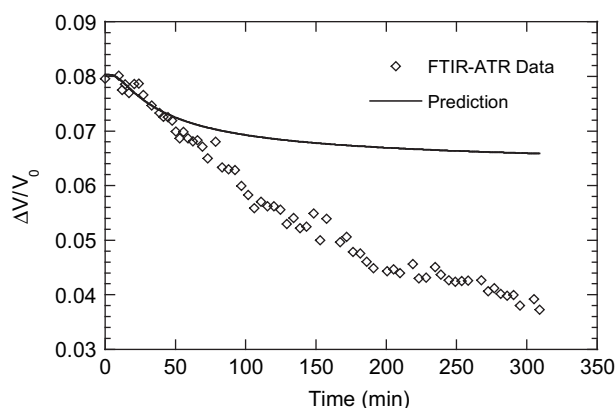


Fig. 12. Prediction of deswelling FTIR-ATR data at activity 0.2 with Eq. (17).  $L = 34.2 \mu\text{m}$  and  $T = 25^\circ\text{C}$ .

According to the physical interpretation of this model, the penetrant population “dissolved” in the matrix, represented by  $C_D^*(t)$ , contributes to the kinetics of polymer swelling. In addition, the holes formed and occupied during sorption, represented by  $C_D^*(t)f_H/1 - f_H$ , also contribute to the swelling kinetics. The swelling induced by the sorption of penetrant can be predicted from  $C_D^*(t)$  using the following expression, assuming that the partial molar volume,  $\bar{V}_{A_D}$ , is constant:

$$\frac{\Delta V}{V_0} = C_D^*(t) \left( 1 + \frac{f_H}{1 - f_H} \right) \frac{\bar{V}_{A_D}}{M_{W_A}} \rho_{\text{poly}} \quad (16)$$

where  $M_{W_A}$  is the molecular weight of acetonitrile and  $\rho_{\text{poly}}$  is the density of CA film. The value of  $\bar{V}_{A_D}$  is assumed to be equal to that in the rubbery state, which was determined to be  $44 \text{ cm}^3/\text{mol}$  from Fig. 4.

$C_D^*(t)$  for acetonitrile in glassy CA at activities 0.1, 0.15, 0.2 and 0.25 were calculated using Eq. (4) and values of the diffusion coefficient at each activity obtained from fitting the FTIR-ATR sorption data. All of the parameters needed are listed above or in Table 1. Eq. (16) was used to predict the swelling as a function of time with the calculated  $C_D^*(t)$ . Eq. (12) was used to convert the time-resolved FTIR-ATR absorbance data to swelling of the polymer for comparison to the prediction. The prediction and the experimental data are shown in Figs. 7–10. From these figures, it is clear

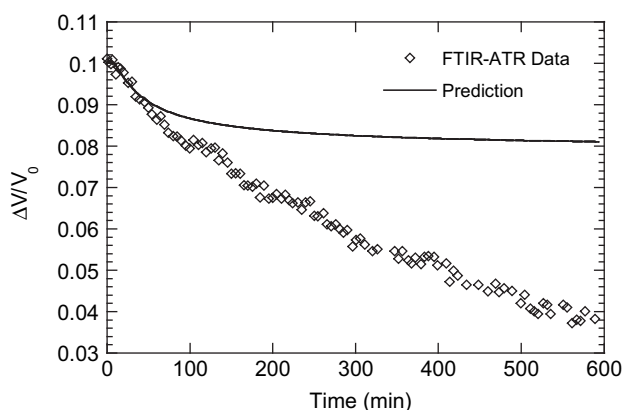


Fig. 13. Prediction of deswelling FTIR-ATR data at activity 0.25 with Eq. (17).  $L = 30.4 \mu\text{m}$  and  $T = 25^\circ\text{C}$ .

that the model, with its associated assumptions, does an excellent job predicting the swelling kinetics.

### 3.4. Study of deswelling kinetics by FTIR-ATR

As stated above in the development of the unified dual mode model for both sorption and desorption, it is assumed that the additional holes formed upon sorption remain during desorption, resulting in additional unrelaxed volume on the time scale of the desorption experiment. The penetrant concentration associated with this additional volume is equal to  $f_H k_D a_d$ . The deswelling kinetics of the polymer can then be written as:

$$\frac{\Delta V}{V_0} = \left( f_H k_D a_d + C_D^*(t) \right) \frac{\bar{V}_{A_D}}{M_{W_A}} \rho_{\text{poly}} \quad (17)$$

Predictions of deswelling kinetics from Eq. (17) are plotted along with deswelling data converted from experimental FTIR-ATR absorbance results at activities 0.15, 0.2 and 0.25 in Figs. 11–13, respectively (deswelling data were not taken at 0.1). It is clear that the unified dual mode model for desorption underpredicts deswelling (less volume collapse than observed) as a function of time. These results suggest that some of the holes formed during sorption close upon desorption. Including this observation into a more robust dual mode model for both sorption/desorption and swelling/deswelling is reserved for future work.

## 4. Conclusion

In this study, time-resolved FTIR-ATR spectroscopy was used to study the swelling and deswelling behavior of cellulose acetate films induced by the sorption and desorption, respectively, of vapor phase acetonitrile. The IR absorbance data for swelling at equilibrium were found to be in excellent agreement with those from direct measurements, further demonstrating that the FTIR-ATR method is a good alternative for studying polymer swelling *in situ*. The hypothesis that swelling kinetics could be predicted from the unified dual mode model for diffusion was validated, however, the mechanism for polymer deswelling is more complicated and will require a reevaluation of the underlying assumptions.

## Acknowledgements

Financial support for J. Guo from the University of Maryland, College Park is gratefully acknowledged.

## References

- [1] Elabd Y, Baschetti MG, Barbari TA. *Journal of Polymer Science: Part B Polymer Physics* 2003;41:2794–807.
- [2] Balik CM, Xu JR. *Journal of Applied Polymer Science* 1994;52:975–83.
- [3] Sammon C, Yarwood J, Everall N. *Polymer* 2000;41:2521–34.
- [4] Baschetti MG, Piccinini E, Barbari TA, Sarti GC. *Macromolecules* 2003;36:9574–84.
- [5] Guo J, Barbari TA. *Macromolecules* 2009;42:5700–8.
- [6] Bohning M, Springer J. *Polymer* 1998;39:5183–95.
- [7] Smith JM, van Ness HC. *Introduction to chemical engineering thermodynamics*. 3rd ed. McGraw-Hill Book Company; 1975.
- [8] Fleming GK. Ph.D. Thesis. University of Texas at Austin; 1988.
- [9] Puleo AC, Paul DR. *Journal of Membrane Science* 1989;47:301–32.
- [10] van Krevelen DW, Hoftyzer PJ. *Properties of polymers—their estimation and correlation with chemical structure*. Amsterdam, Oxford and New York: Elsevier; 1976.
- [11] Carlton Jr. TA, Aramayo GA. “Stability of small plastic cylinders subjected to internal pressure and axial compression”. Technical Report submitted to George E. Marshall Space Flight Center, NASA. Accession No. N65-34391, University of Alabama; 1965.